

University of California
Ernest O. Lawrence
Radiation Laboratory

TWO-WEEK LOAN COPY

*This is a Library Circulating Copy
which may be borrowed for two weeks.
For a personal retention copy, call
Tech. Info. Division, Ext. 5545*

**K^+ p INTERACTIONS AT 2 BeV/c - ELASTIC
SCATTERING AND TOTAL CROSS SECTIONS**

Berkeley, California

DISCLAIMER

This document was prepared as an account of work sponsored by the United States Government. While this document is believed to contain correct information, neither the United States Government nor any agency thereof, nor the Regents of the University of California, nor any of their employees, makes any warranty, express or implied, or assumes any legal responsibility for the accuracy, completeness, or usefulness of any information, apparatus, product, or process disclosed, or represents that its use would not infringe privately owned rights. Reference herein to any specific commercial product, process, or service by its trade name, trademark, manufacturer, or otherwise, does not necessarily constitute or imply its endorsement, recommendation, or favoring by the United States Government or any agency thereof, or the Regents of the University of California. The views and opinions of authors expressed herein do not necessarily state or reflect those of the United States Government or any agency thereof or the Regents of the University of California.

UNIVERSITY OF CALIFORNIA

Lawrence Radiation Laboratory
Berkeley, California

AEC Contract No. W-7405-eng-48

K^+ INTERACTIONS AT 2 BeV/c -- ELASTIC SCATTERING
AND TOTAL CROSS SECTIONS

W. Chinowsky, G. Goldhaber, S. Goldhaber,
T. O'Halloran and B. Schwarzschild

November 1964

K^+ p Interactions at 2 BeV/c - Elastic Scattering and Total Cross Sections*W. Chinowsky, G. Goldhaber, S. Goldhaber, T. O'Halloran,[†] and B. SchwarzschildLawrence Radiation Laboratory and Department of Physics
University of California
Berkeley, California

Study of 1.96 BeV/c K^+ p interactions in the Brookhaven 20-inch liquid hydrogen bubble chamber has yielded a measurement of the elastic scattering cross section $\sigma = 7.5 \pm 0.7$ mb. A fit to the differential cross section vs momentum transfer of the form $\sigma_0 e^{-\alpha t}$ gives, for the interval $0.01 (\text{BeV}/c)^2 < t < 0.60 (\text{BeV}/c)^2$, $\alpha = 3.1 \pm 0.3 (\text{BeV}/c)^2$ and $\sigma_0 = 4.8 \pm 0.6$ mb. The total cross section obtained is 19.4 ± 2.0 mb with single pion production dominant.

I. INTRODUCTION

At energies sufficiently above the threshold for inelastic processes, all elastic scattering shows a characteristic large forward "diffraction" peak. It is thought that the characteristics of the diffraction scattering may not depend on the properties of the particular particles involved. Unified descriptions of high energy elastic scattering have been suggested by various authors and asymptotic formulas have been constructed.¹ To determine the validity of such descriptions, it is of interest to compare the diffraction scattering of various particles on protons, in the same regime of momentum transfer. We present here the results of a study of K^+ p elastic interactions in the 20-inch hydrogen bubble chamber exposed to a separated K^+ beam of momentum 1.96 ± 0.02 BeV/c from the Brookhaven A.G.S.² We include also cross sections for the various inelastic reactions.

* Work done under the auspices of the U. S. Atomic Energy Commission

[†] Now in the Department of Physics, Harvard University

II. THE TOTAL ELASTIC CROSS SECTION

All two-prong events were measured on digitized projectors and analyzed with the reconstruction and fitting program PACKAGE.³ After correcting for scanning biases and ambiguous interpretations we arrive at a total number of elastic scattering events $N_T = 1094$ occurring within a predetermined fiducial volume of the hydrogen chamber. (For details see Appendix). In the same volume were 164 τ decays from which we find the incident K^+ flux.⁵ From these data we evaluate the total elastic K^+p scattering cross section

$$\sigma_E = 7.5 \pm 0.7 \text{ mb}$$

where the error is statistical. Cook et al.⁶ have reported a total elastic cross section of 5.6 ± 0.4 mb at 1.97 BeV/c.

III. DIFFERENTIAL CROSS SECTION

The observed angular distribution of the elastic scattering is shown in Figs. 1 and 2. We find the expected predominant diffraction peak in the forward direction. In the backward hemisphere the data are too sparse for detailed study. No attempt is made at a phase shift analysis. Guided by "Regge" theory and an optical model discussed below,⁷ we seek to fit the observed angular distribution, below some upper limit of the momentum transfer squared t , by an exponential form

$$\frac{d\sigma}{d\Omega} = \sigma_0 e^{-\alpha t}$$

where $t \equiv +2\bar{P}^2 (1 - \cos\bar{\theta})$, and \bar{P} and $\bar{\theta}$ are respectively the c.m. momentum and scattering angle. This is seen in Fig. 1 to fit the data well in the forward hemisphere. Because the average measurement error of t is not negligibly small compared with the width of the rapidly decreasing angular distribution, it is incorrect

to obtain α merely from the slope of a least squares straight line fit to the histogram of Fig. 1. The finite momentum transfer resolution results in a net shift of the measured distribution relative to the true distribution in the direction of increasing t , that is, in the direction of decreasing cross section. We therefore obtain α^* , the best estimate of α , from a maximum likelihood procedure which takes explicit account of the measurement errors and makes optimum use of the experimental information. The likelihood function has the form

$$L(\alpha) = \prod_j P_j(t_j, \sigma_j, \alpha) \quad (2)$$

where \prod_j is a product over all events in the t interval t_{\min} to t_{\max} being fitted to $e^{-\alpha t}$; t_j and σ_j are respectively the measured t (from the kinematic fitting program) and its uncertainty for the j^{th} event. For convenience we take the error distribution in t to be a truncated Gaussian, cut off on each side at either three standard deviations or the kinematic limit, whichever is reached first, and normalized accordingly. Then

$$P(t, \sigma, \alpha) = \frac{1}{N_\sigma(\alpha)} \int_{\xi = \max(0, t-3\sigma)}^{\min(\xi_{\max}, t+3\sigma)} Q(t, \xi, \sigma, \alpha) d\xi \quad (3)$$

where ξ is the true value of t for the j^{th} event, and $\xi_{\max} = 2.74$ BeV/c is the kinematic upper limit of ξ at 1.96 BeV/c. Here $\frac{1}{N_\sigma(\alpha)} \int Q(t, \xi, \sigma, \alpha) d\xi dt$ is the probability that for a sample of events with arbitrary cutoffs t_{\min} , t_{\max} an event will have true momentum transfer squared in the interval $d\xi$, and measured momentum transfer squared in the interval dt . Q has the form

$$Q(t, \xi, \sigma, \alpha) = e^{-\alpha \xi} \frac{e^{-\frac{1}{2} \left(\frac{t-\xi}{\sigma} \right)^2}}{M(\sigma, \xi)} \quad (4)$$

The normalization factors are

$$M(\sigma, \xi) = \int_{\tau = \max(0, \xi - 3\sigma)}^{\min(\xi_{\max}, \xi + 3\sigma)} e^{-\frac{1}{2} \left(\frac{\tau - \xi}{\sigma} \right)^2} d\tau \quad (5)$$

and

$$N_{\sigma}(\alpha) = \int_{t = t_{\min}}^{t_{\max}} \int_{\xi = \max(0, t - 3\sigma)}^{\min(\xi_{\max}, t + 3\sigma)} Q(t, \xi, \sigma, \alpha) dt d\xi \quad (6)$$

This maximum likelihood procedure yielded the results shown in Table I for three different intervals of momentum transfer.

TABLE I. Results of Fitting Elastic Angular Distribution to $e^{-\alpha t}$

	Interval I	Interval II	Interval III
$t_{\min} (\text{BeV } c)^2$	0.0103 ($\bar{\theta}=7^{\circ}$)	0.0103	0.025 ($\bar{\theta}=11^{\circ}$)
t_{\max}	0.6	1.0	0.4
N(number of events)	510	590	394
$\alpha^* \pm \Sigma (\text{BeV } c)^{-2}$	3.1 ± 0.3	2.9 ± 0.14	3.3 ± 0.5
expected Σ	0.28	0.17	0.48
$P(\chi^2)$	0.7	0.4	---

If $L(\alpha)$ has the Gaussian form $L(\alpha) \sim \exp\left[-\frac{1}{2} \left(\frac{\alpha - \alpha^*}{\Sigma}\right)^2\right]$ expected for good statistics, $\ln L$ will have the parabolic form $\ln L = -\frac{1}{2} \left(\frac{\alpha - \alpha^*}{\Sigma}\right)^2 + \text{const.}$ Then Σ , the R.M.S. variance of L , is given by the half width of the parabola at $\ln L(\alpha) = \ln L(\alpha^*) - \frac{1}{2}$. The uncertainties, Σ , quoted in Table I were

determined in this way. The likelihood curve for Interval I is shown in Fig. 3. It is seen to be parabolic, as are also the curves $\ln L(\alpha)$ for the other two intervals.

A peculiarity of the exponential hypothesis is that the numerical value of $\ln L(\alpha^*)$ depends only on α^* and so cannot be used as a measure of goodness of fit. We therefore calculated χ^2 's for intervals I and II by comparing the histogram of Fig. 1 with $\sigma_0 e^{-\alpha^* t}$. The forward scattering cross sections, σ_0 , were obtained from the fractional cross sections for the intervals considered, and are given in Table II. The α^* 's and χ^2 's are of course independent of the overall normalization.⁵ $P(\chi^2)$, the probability the χ^2 would be greater than that calculated if the hypothesis is correct, is listed in Table I. $\sigma_0 e^{-\alpha^* t}$ for Interval I has been superimposed on Fig. 1. As an additional measure of goodness of fit we calculated the expected variance of α^*

$$\text{expected } \Sigma = \frac{1}{N} \left[\int_{t=t_{\min}}^{t_{\max}} \frac{1}{P} \left(\frac{\partial P}{\partial \alpha} \right)_{\alpha^*}^2 dt \right]^{\frac{1}{2}} \quad (7)$$

using the approximation

$$P(t, \sigma, \alpha) \approx \frac{\alpha}{\left[e^{-\alpha t_{\min}} - e^{-\alpha t_{\max}} \right]} e^{-\alpha t} \quad (8)$$

A fit to a distribution with the likelihood function of an incorrect hypothesis generally produces Σ larger than expected. In this respect the expected Σ 's shown in Table I indicate a good fit for all three intervals.

Using α^* for Interval I we obtain the forward differential cross section

$$\sigma_0 = 4.8 \pm 0.6 \frac{\text{mb}}{\text{sr}}$$

From the optical theorem, with total cross section $\sigma_T = 19.4 \pm 2.0$ mb, obtained from the present experiment, we have

$$\sigma_0 \geq 4.3 \pm 0.9 \frac{\text{mb}}{\text{sr}}$$

It is seen that the forward scattering amplitude is predominantly imaginary as expected, and consistent with being purely imaginary. We have compared our data with a purely imaginary high energy scattering amplitude of the form

$$f(\bar{\theta}) = \frac{ik}{\sqrt{\pi}} \left[a_0 e^{-\frac{1}{2} A_1 t} + C(E) \pm b_0(E) e^{-\frac{1}{2} B_1 (\xi_{\text{max}} - t)} \right] \quad (9)$$

suggested by Minami⁷ to explain both the increase of α with energy for some systems (e.g. K^+p , pp) and the absence of this Regge theory predicted effect for others (e.g. πp , $\bar{p}p$). In contrast to Regge theory A_1 is here taken to be energy independent, as are a_0 and B_1 . From higher energy K^+p elastic scattering data, then, Minami finds

$$a_0 = 18.2 \frac{(\text{mb})^{\frac{1}{2}}}{\text{BeV}/c} \quad \text{and} \quad A_1 = 5.6 (\text{BeV}/c)^{-2}$$

Using these values we conclude that Eq. (9), for which Minami finds evidence in the region 7 to 15 BeV/c of K^+p elastic scattering, is inconsistent with our data at 2 BeV/c.

It is interesting to note that the exponential dependence on t ,

$$\frac{d\sigma}{d\Omega} = \sigma_0 e^{-\alpha t} \quad (1)$$

follows also from an optical model in which it is assumed that the transmitted

amplitude $a(b)$, for impact parameter b , is given by

$$1 - a(b) = (A + Bi)e^{-b/\langle b^2 \rangle} \quad (10)$$

Setting $a(b) = e^{i\chi(b)}$ in

$$f(\bar{\theta}) = \frac{k}{i} \int_{b=0}^{\infty} J_0(2kb \sin \frac{\bar{\theta}}{2}) \{e^{i\chi(b)} - 1\} b db \quad (11)$$

it follows that

$$\frac{d\sigma}{d\Omega} = \sigma_0 e^{-\frac{1}{2} \langle b^2 \rangle t} \quad (12)$$

where $\langle b^2 \rangle = 2\alpha$ is a measure of the mean square radius of the K^+p interaction. The region of validity of the approximation Eq. (11) is $\bar{\theta} \lesssim 23^\circ$.

The results, in terms of both parametrizations, are shown in Table II, where they are also compared with those of Cook et al.⁶

For comparison we include in Table II the results of various elastic scattering experiments of K^- , π^+ , π^- , p , and \bar{p} on protons at approximately the same total barycentric energy, parametrized in terms of α .

TABLE II. Elastic diffraction peaks of various systems at $E_{cm} \approx 2.2$ BeV fitted to $\frac{d\sigma}{d\Omega} = \sigma_0 e^{-\alpha t} = \sigma_0 e^{-\frac{1}{2} \langle b^2 \rangle t}$

Experiment	P_{LAB} (BeV/c)	Interval fitted $t \ll$	α (BeV/c) ⁻²	$\sqrt{\langle b^2 \rangle}$ (f)	σ_0 (mb/sr)
K^+p this exp't.	1.96	1.0 (BeV/c) ⁻²	$2.9 \pm .14$	$.48 \pm .01$ (a)	4.58
K^+p "	1.96	0.6	$3.1 \pm .3$	$.49 \pm .02$	$4.8 \pm .6$
K^+p "	1.96	0.4	$3.3 \pm .5$	$.51 \pm .035$	
K^+p (c)	1.97	0.21	3.9 ± 1.2	$.55 \pm .15$	$3.6 \pm .2$
K^-p (d)	2.00	0.4	9.1 (b)	.84	12.91
K^-p (e)	1.95	0.6	$7.9 \pm .6$	$.78 \pm .03$	$12.5 \pm 1.$
π^+p (f)	2.02	0.4	$5.7 \pm .4$		
π^+p (g)	2.0		$5.0 \pm .4$		
π^-p (f)	2.01	0.4	$7.8 \pm .2$		
π^-p (e)	1.95	0.36	$8.1 \pm .2$	$.79 \pm .1$	$10.4 \pm 2.$
π^-p (h)	2.05	0.25	$7.84 \pm .7$		
pp (i)	1.45	0.15	10. (b)		
$\bar{p}p$ (j)	1.61	0.17	13. (b)		

Footnotes to Table II:

- (a) Uncertainties in $\sqrt{\langle b^2 \rangle}$ propagated from α errors. This is justified if $L(\alpha)$ is Gaussian as indicated by Fig. 3 and similar $\log L(\alpha)$ curves for our other fitted t intervals.
- (b) Our fits to data presented by the quoted authors.
- (c) See Reference 6.
- (d) See Reference 8.
- (e) See Reference 9.
- (f) See Reference 10.
- (g) See Reference 11.
- (h) See Reference 12.
- (i) See Reference 13.
- (j) See Reference 14.

It is quite clear that the simplest unified models of the diffraction scattering fail at this energy. Some regularity appears, in that the positive particle in all cases shows a smaller slope, with approximately a constant difference $(\alpha_- - \alpha_+) \approx 3^{-4} (\text{BeV}/c)^{-2}$.

IV. INELASTIC CROSS SECTIONS

In Table III are listed the partial cross sections for all open channels.² Identifications were made on the basis of kinematic fit and bubble density estimates. The quoted errors are statistical only and do not include uncertainties due to incorrect identification, believed small compared to the purely statistical uncertainties. Detailed characteristics of these reactions are discussed elsewhere.^{2,4} The Λ^0 production cross section is an upper limit, no hyperons having been observed.

TABLE III. Cross sections observed for the K^+p interaction at 1.96 BeV/c.

Reaction product	Cross section (mb)
K^+p elastic	7.5 ± 0.7
$K^0\pi^+p$	4.6 ± 0.6
$K^+\pi^0p$	2.0 ± 0.3
$K^+\pi^+n$	1.6 ± 0.3
$K^+\pi^-p\pi^+$	1.7 ± 0.2
$K^0\pi^0p\pi^+$	1.3 ± 0.2
$K^0\pi^+n\pi^+$	0.33 ± 0.1
$K^+\pi^0n\pi^+$	~ 0.3
$K^+\pi^-\pi^0\pi^+p$	0.05 ± 0.02
$K^0\pi^+\pi^-\pi^+p$	0.02 ± 0.01
$K^+\pi^-\pi^+\pi^+n$	0.01 ± 0.006
$K^+K^+\Lambda$	$\lesssim 0.01$
σ_{total}	19.4 ± 2.0

APPENDIXA. Corrections to the Selection of Elastic Scattering Events

Two major difficulties arise in the selection of the elastic events:

- (1) a low efficiency for finding events with short recoil protons, and
- (2) distinguishing between elastic scattering and π^0 production $K^+ p \longrightarrow K^+ p \pi^0$.

To eliminate the first, a minimum projected track length was determined which made the scanning efficiency independent of track length. This determined a minimum scattering angle cutoff $\bar{\theta} = 7^\circ$ corresponding to $t \cong .01 \left(\frac{\text{BeV}}{c}\right)^2$, as well as a 55° maximum cutoff in the azimuthal angle ϕ between the plane of the outgoing tracks and the plane of the four cameras (the plane of zero "dip" angle). This restriction on ϕ also eliminates steep tracks making the evaluation of relative bubble densities more reliable.

Events satisfying these criteria and the kinematics of elastic scattering were usually kinematically consistent also with the reaction $K^+ + p \longrightarrow K^+ + \pi^0 + p$ and often with the reactions $K^+ + p \longrightarrow \pi^+ + p + K^0$ and $K^+ + p \longrightarrow K^+ + \pi^+ + n$. In all cases π^+ production could be distinguished from elastic scattering by observation of track bubble densities. This procedure was not useful for the hypothesis of single π^0 production if neither outgoing track had momentum between about 400 and 1300 MeV/c or stopped in the chamber. The ambiguous $K^+ p \pi^0$ fits, however, almost invariably posited a π^0 of $\cos \bar{\theta} < -0.95$ and $\bar{P} < 100$ MeV/c. Since this pattern was also exhibited by the $K^+ p \pi^0$ fits rejected on the basis of bubble density and was inconsistent with smooth extrapolation of the distribution of uniquely identified $K^+ p \pi^0$ events, it is likely that such fits are spurious, resulting from inaccuracies of momentum measurement. The 80 ambiguous events of this type were thus included in the elastic scattering group. In this way 636 events were accepted as elastic scatters. The χ^2 distribution is

in good agreement with that expected for four constraint events. Of the two-prong events which failed to fit the hypotheses of either two or three particles in the final state, 34 were classified to have two neutral particles in the final state and 49 were immeasurable for technical reasons. The four-body final states were identified by computing the missing mass from the unbalance in momentum and energy. The number of events whose missing mass is consistent with either a neutral K^* or a neutral N^* is in agreement with the number expected from charge independence and the number of such resonant states found in the analysis of the four-charged-prong events.⁴ Assuming the observed ratio of elastic to inelastic two-prong events to be the same for the immeasurable events, we take 22 of these to be elastic in our cross section determination.

Extrapolating the observed distribution of Fig. 1 to zero momentum transfer assuming for the differential cross section an exponential dependence $e^{-\alpha t}$, which is in excellent agreement with observation for $t < 0.6 \text{ BeV}/c$, gave 19 events to be added to the sample. Correcting for the azimuthal angle cutoff and the estimated fraction of elastic events which were immeasurable, we arrive at a total $N_T = 1094$ events for all t and ϕ .

B. Pion Contamination

We evaluated the π^+ contamination in the beam by fitting all four-prong events to the hypotheses of an incident π^+ . Four-prong events were used because the $\pi^+ p$ cross section for this topology is about three times as great as that for $K^+ p$, thus giving an enriched sample of beam contaminants. Only one event satisfying entrance angle and momentum criteria was found to favor incoming pion kinematics, yielding an estimated π^+ beam contamination of $0.25^{+0.5}_{-0.25}\%$ which we neglect. This estimate is consistent with that obtained from the measured $K-\pi$ separation² in the beam.

ACKNOWLEDGEMENTS

It is a pleasure to acknowledge the hospitality and helpfulness of the Brookhaven National Laboratory Staff. Our particular thanks go to Dr. Ralph Shutt and the bubble chamber operating staff, and to Dr. K. Green and the A.G.S. operations group. Finally we wish to thank our scanning, measuring, data processing and secretarial personnel at Berkeley for their devoted and indispensable efforts.

REFERENCES

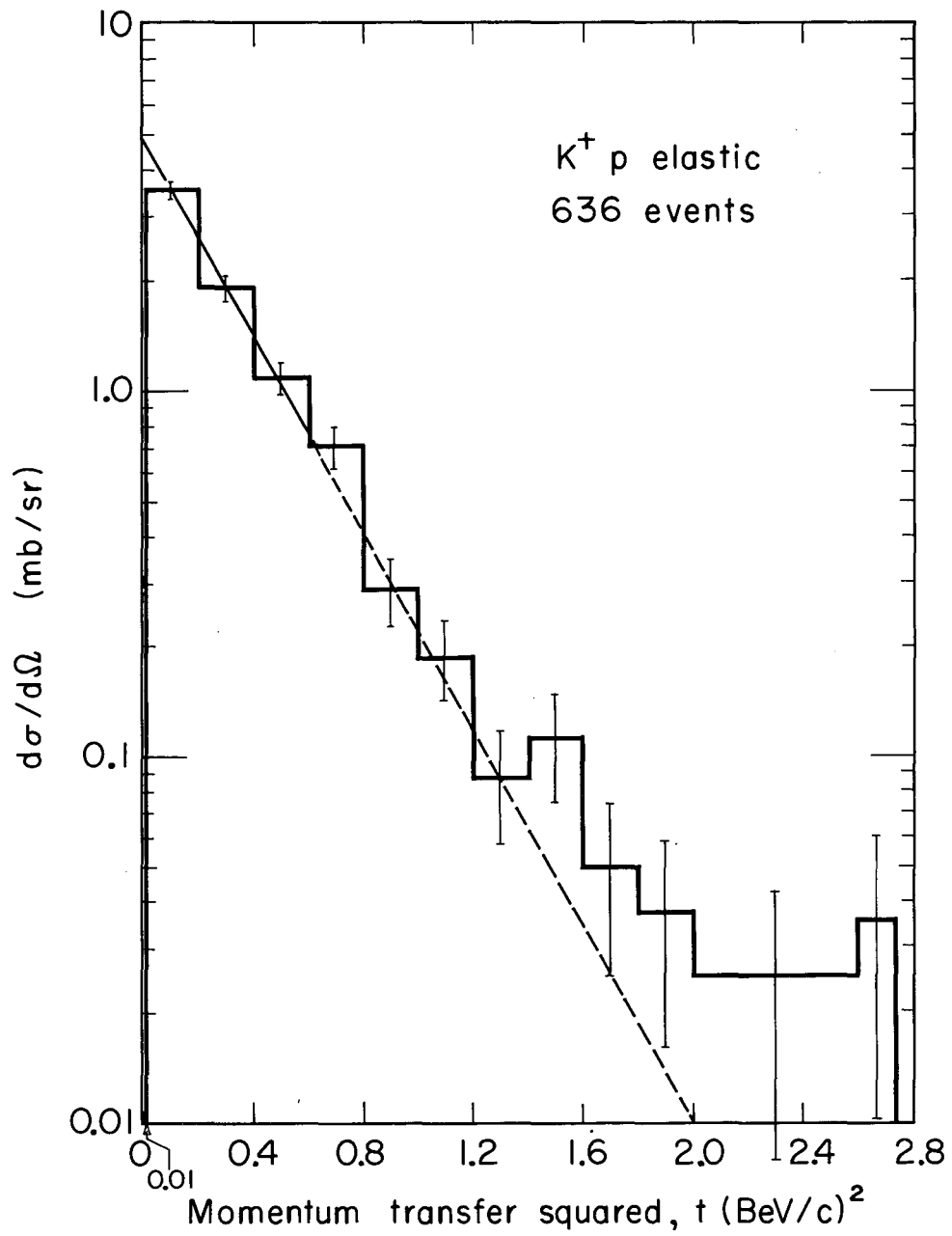
1. S. Fernbach, R. Serber, and T. B. Taylor, Phys. Rev. 75, 1352 (1949);
P. T. Matthews and A. Salam, Nuovo Cimento XXI, 127, 823 (1961);
R. Serber, Phys. Rev. Letters 10, 357 (1963);
S. Minami (see Reference 7);
G. F. Chew, S. C. Frautschi, Phys. Rev. Letters 1, 394 (1961);
S. C. Frautschi, M. Gell-Mann, and F. Zachariasen, Phys. Rev. 126,
2204 (1962);
G. F. Chew, S. C. Frautschi, and S. Mandelstam, Phys. Rev. 126,
1202 (1962);
R. Blankenbecler and M. L. Goldberger, Phys. Rev. 126, 766 (1962);
B. M. Udgaonkar, Phys. Rev. Letters 8, 142 (1962).
2. T. A. O'Halloran, Jr. UCRL-11068 (Thesis), (1963), Lawrence Radiation
Laboratory, Berkeley, California.
3. A. H. Rosenfeld, UCRL-9099 (1961), Lawrence Radiation Laboratory,
Berkeley.
4. G. Goldhaber, S. Goldhaber, W. Chinowsky, W. Lee, and T. O'Halloran,
Physics Letters 6, 62 (1963).
5. All three-prong K^+ decays are included in this group. Branching ratios
of Roe et al. (Phys. Rev. Letters 7, 346 (1961)) with corrections for
Dalitz pair decays were used in determining cross sections in this
paper. Very recently two new determinations of the τ branching ratio
have appeared (Callahan et al. (1964) and Shaklee et al. (1964) as
quoted in Rosenfeld et al., UCRL-8030, I, (1964), Lawrence Radiation
Laboratory, Berkeley, California). Comparing all available results

Rosenfeld et al. find a τ branching ratio of $.055 \pm .001$ as compared with $.057 \pm .003$ of Roe et al. used in the present paper. The effect of this would be to decrease all the cross sections given in the present paper by a factor 59/61.

6. V. Cook, D. Keefe, L. T. Kerth, P. G. Murphy, W. A. Wenzel and T. F. Zipf, Phys. Rev. 129, 2743 (1963).
7. S. Minami, Phys. Rev. 135, B1263 (1964).
8. R. Crittenden, H. Martin, W. Kernan, L. Liepuner, A. C. Li, F. Ayer, L. Marshall, and M. L. Stevenson, Phys. Rev. Letters 12, 429 (1964).
9. V. Cook, B. Cork, T. F. Hoang, D. Keefe, L. Kerth, W. Wenzel and T. Zipf, Phys. Rev. 123 320 (1961).
10. D. E. Damouth et al., Techn. Report No. 12 (1963) University of Michigan, Ann Arbor.
11. V. Cook, B. Cork, W. Holly and M. Perl, Phys. Rev. 130, 762 (1962).
12. L. D. Jacobs and D. Miller, Lawrence Radiation Laboratory, Berkeley, private communication.
13. T. Morris, E. Fowler, and J. Garrison, Phys. Rev. 103, 1472 (1956).
14. G. Lynch, R. Foulks, G. Kalbfleisch, S. Limentani, J. B. Shafer, M. L. Stevenson, and N. Xuong, Phys. Rev. 131, 1276 (1963).
15. R. J. Glauber, Lectures in Theoretical Physics I, Boulder 1958, Interscience, N. Y. (1959).

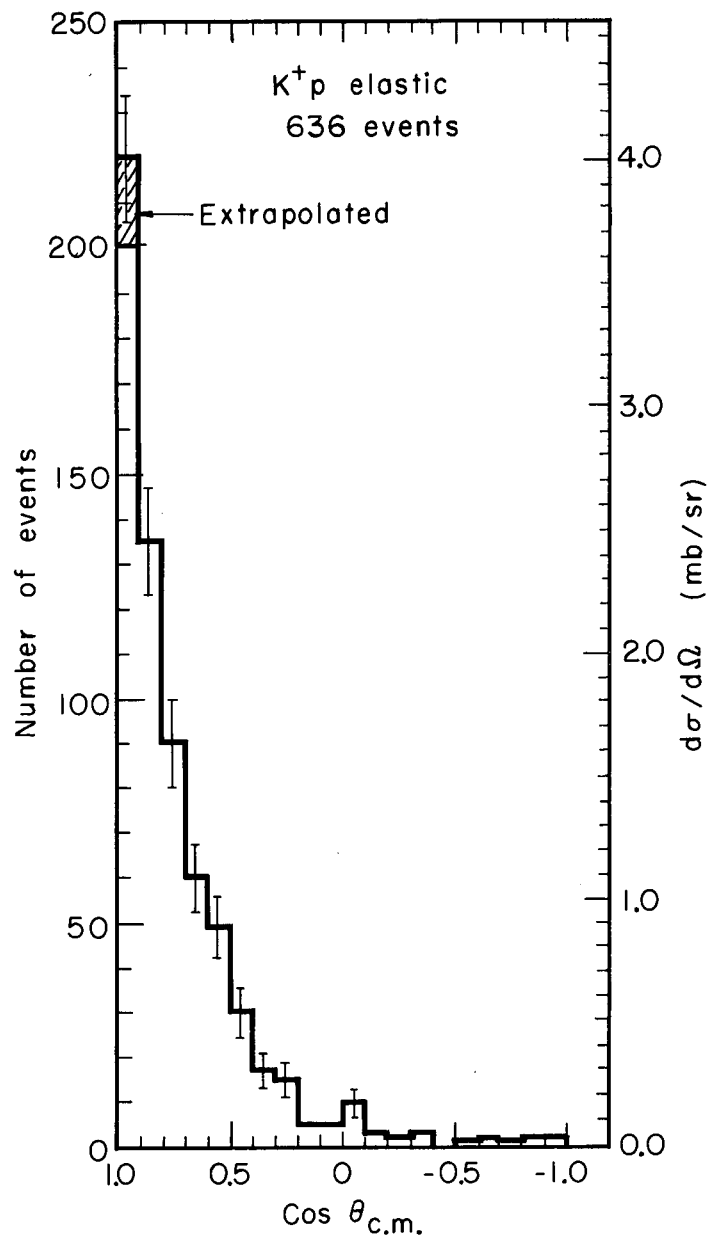
FIGURE CAPTIONS

- Fig. 1. Logarithmic distribution of 636 elastic scattering events vs momentum transfer squared t . The straight line shows $d\sigma/d\Omega = \sigma_0 \exp(-\alpha^* t)$ where $\alpha^* = 3.1 (\text{BeV}/c)^{-2}$ is the maximum likelihood estimator (Eqs. 2-6) for interval I ($.01 \leq t \leq .6 [\text{BeV}/c]^2$), and $\sigma_0 = 4.8 \text{ mb/sr}$. The line is dashed in the extrapolated region beyond the fitted interval.
- Fig. 2. Angular distribution of 636 elastic scattering events. Shaded area indicates events deduced by extrapolation below cutoff $\theta_{\text{cm}} = 7^\circ$, assuming angular distribution $\sim \exp(-\alpha t)$.
- Fig. 3. Logarithm of likelihood function $L(\alpha)$ (Eqs. 2-6) used to fit Interval I ($.01 \leq t \leq .6 [\text{BeV}/c]^2$) to the hypothesis $d\sigma/d\Omega \sim \exp(-\alpha t)$. The estimator α^* is obtained from the maximum of the likelihood function, and Σ , the R.M.S. variance of $L(\alpha)$ is the half width of $\ln L(\alpha)$ at $\ln L(\alpha^*) - \frac{1}{2}$.



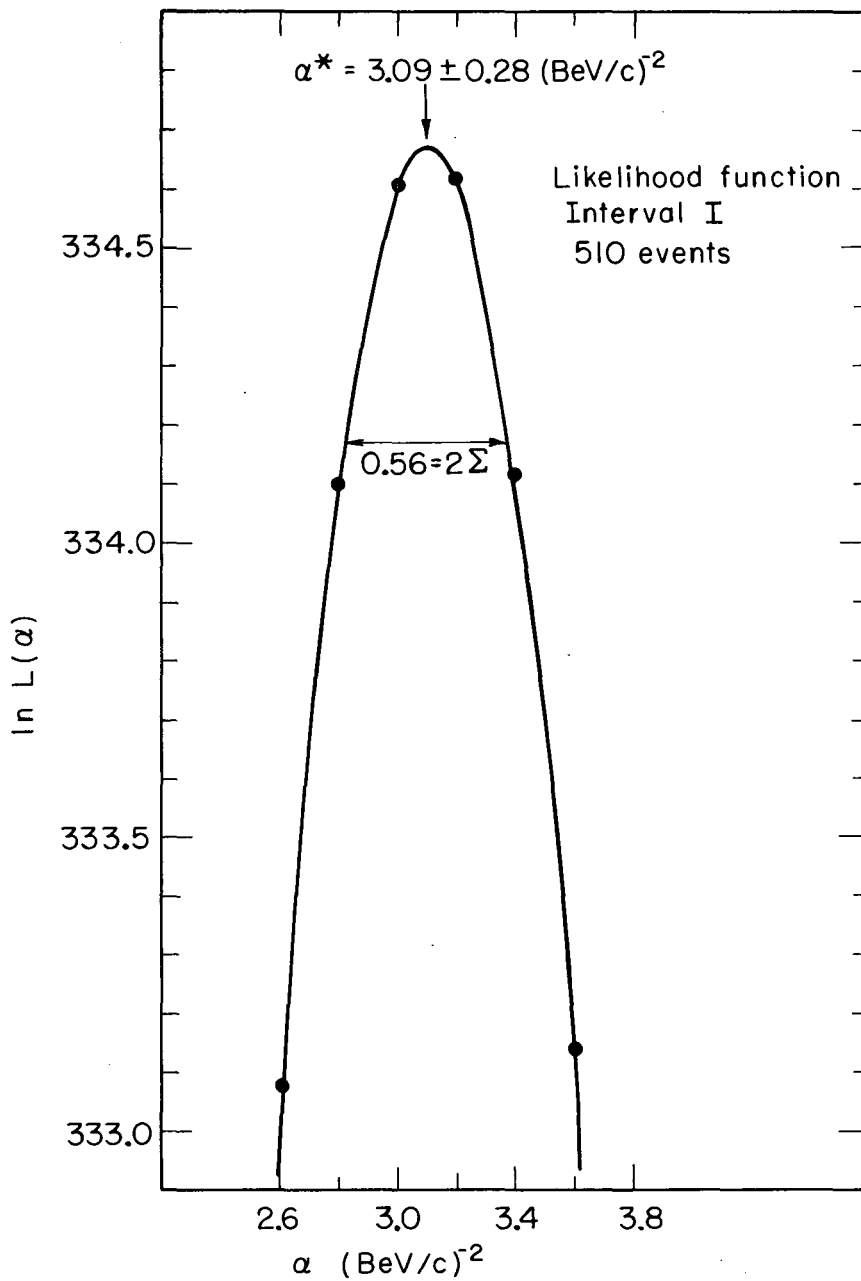
MUB-4008

Fig. 1



MUB-4356

Fig. 2



MUB-4010

Fig. 3

This report was prepared as an account of Government sponsored work. Neither the United States, nor the Commission, nor any person acting on behalf of the Commission:

- A. Makes any warranty or representation, expressed or implied, with respect to the accuracy, completeness, or usefulness of the information contained in this report, or that the use of any information, apparatus, method, or process disclosed in this report may not infringe privately owned rights; or
- B. Assumes any liabilities with respect to the use of, or for damages resulting from the use of any information, apparatus, method, or process disclosed in this report.

As used in the above, "person acting on behalf of the Commission" includes any employee or contractor of the Commission, or employee of such contractor, to the extent that such employee or contractor of the Commission, or employee of such contractor prepares, disseminates, or provides access to, any information pursuant to his employment or contract with the Commission, or his employment with such contractor.

